Recovery of pointwise sources or small inclusions in 2D domains and rational approximation

L Baratchart[1], **A Ben Abda**[2], **F Ben Hassen**[2,3] **and J Leblond**[1,4]

[1] INRIA, BP 93, 06902 Sophia-Antipolis Cedex, France
[2] ENIT-LAMSIN, BP 37, 1002 Tunis Belvédère, Tunisia
[3] Institut für Numerische und Angewandte Mathematik, University of Göttingen, Lotzestr. 16–18, 37083 Göttingen, Germany

Abstract
We consider the inverse problems of locating pointwise or small size conductivity defaults in a plane domain, from overdetermined boundary measurements of solutions to the Laplace equation. We express these issues in terms of best rational or meromorphic approximation problems on the boundary, with poles constrained to belong to the domain. This approach furnishes efficient and original resolution schemes.

1. Introduction: models

We approach here the classical inverse problem of determining, from boundary Cauchy data of solutions to the Laplace equation, hidden pointwise or small size conductivity defaults in a plane domain.

A first practical motivation lies with the inverse source problem in $\mathbb{R}^3$ of locating epileptic foci in the human brain, the so-called *inverse electroencephalography* (EEG) problem. Epilepsy is related to electrical discharges that originate from a small volume, hence epilepsy foci are usually approximated by pointwise current dipoles. In that case a classical though strongly simplified model is the spherical one [36] that we sketch below to lend perspective to the discussion. There, the inverse source problem consists in determining the location within a ball of a finite number of dipoles together with their moments from available data on the sphere. Actually, this in *not* the question treated in the present paper where only planar domains are considered. However, beyond the interest of the two-dimensional (2D) case in its own right (particularly for 3D axisymmetric situations), the approach that we propose, in order to recover *both* monopolar and dipolar pointwise sources in a plane domain, provides a platform to handle the problem in a ball of $\mathbb{R}^3$ by considering a family of 2D problems on planar cross sections of the ball. Note that this requires no symmetry assumptions and could be further extended to more general 3D volumes surrounded by parametrized surfaces [9].

[4] Author to whom any correspondence should be addressed.

Further motivation arises from the need to detect regular small size inclusions scattered in a planar matrix phase of known background conductivity. The non-destructive techniques used for recovering the conductivity distribution inside a body from boundary measurements of the voltage potential and the current flows are called impedance electrical tomography (EIT). This method has a wide range of applications especially in medical imaging and nondestructive control of materials, see [25]. Impedance tomography gives rise to nonlinear and severely ill-posed problems. The situation changes when we have *a priori* knowledge about the conductivity, which allows one to determine other specific features of the medium, with high resolution.

We consider here two particular geometrical elliptic inverse problems, related to the Laplace operator, consisting, as described above, in recovering conductivity defaults (either sources or inhomogeneities) from boundary measurements. We approach and solve them in 2D, using approximation schemes for complex variable functions built on the boundary data. The originality of this work is mainly in linking these mathematical problematics together, leading to new and costless algorithms to solve for Laplace inverse problems; in particular, they do not require multiple resolution of the associated direct problem. Note that these are *theoretical* (as well as constructive) approximation algorithms in the sense that convergence properties are available for the classes of functions arising here, which, together with their numerical efficiency, is an advantage over other approaches (such as classical discrete least-squares for pointwise boundary data computed with finite elements). In fact, we propose here a somewhat dual approach that consists in best approximating (functions interpolated on) the boundary data rather than the involved Laplace operator, on appropriate classes of harmonic or analytic functions whose singularities (poles) describe those of the expected solution in a suitable way, in order to make the problem well posed and the scheme convergent.

1.1. Overview

This paper is thus devoted to the presentation of a theoretical and constructive inversion process exploiting the best meromorphic and rational approximation of boundary data for two particular elliptic inverse problems, described in sections 1.2 and 1.3, with some survey of available related results. In section 2.2, we give more details about our inverse source problem and we express it as a problem of locating the singularities of a complex-valued function from knowledge on the boundary, using harmonic conjugation. In section 2.3, we make use of an asymptotic expansion for the difference between the solution to (5) and that of the associated homogeneous problem whose dominant term is a rational function. In sections 3.1 and 3.2, we present the construction and some properties of the best $L^2(T_2)$ and $L^\infty(T_2)$ meromorphic approximants and the behaviour of their poles with respect to the singularities of the function to be approximated. We then show in section 4.1 how they are related to the source parameters and give some numerical results to check the accuracy of the proposed method. This is then applied in section 4.2 to the problem of identification of small size inclusions, where computational experiments tend to demonstrate its viability to locate such inhomogeneities.

1.2. Pointwise sources and inverse EEG problem

The so-called *spherical model* of the head consists of a ball $\Omega \subset \mathbb{R}^3$ which is assumed to be made up of three (or more) disjoint homogeneous connected layers (corresponding to scalp, skull and brain) denoted by $\Omega_i, i = 0, 1, 2$, with spherical boundaries and constant

conductivities σ_i. We assume that Ω_0 (the brain) is the unit ball B_3 of $\mathbb{R}^3$, whose boundary ∂B_3 is denoted by T_3, and we let the source term F be of the form

$$F = \sum_{j=1}^{m_1} \lambda_j \delta_{S_j} + \sum_{k=1}^{m_2} p_k \cdot \nabla \delta_{C_k}, \tag{1}$$

with $S_j, C_k \in \Omega_0$, $\lambda_j \in \mathbb{R}$, $p_k \in \mathbb{R}^3$. The steady-state electric potential u associated with the current flux ϕ and the source term F [27, 36] is, in a sense to be clarified presently, a solution of

$$\begin{cases} -\nabla \cdot (\sigma \nabla u) = F \text{ in } \Omega \\ \sigma \dfrac{\partial u}{\partial \nu}_{|\partial \Omega} = \phi \end{cases} \tag{2}$$

where ν represents the outward unit normal vector to $\partial \Omega$, and σ is a piecewise constant conductivity which is equal to σ_i on Ω_i, $i = 0, 1, 2$. Assume that additional measurements of the solution are available on a part of the boundary $\gamma_* \subset \partial \Omega$, where we have $u_{|\gamma_*} = g$. From measurements of g on γ_* and ϕ on $\partial \Omega$, the inverse EEG problem is that of finding F verifying (1) (supported in $\Omega_0 = B_3 \subset \Omega$) such that (2) holds.

The identifiability result [29, theorem 1] ensures that the above inverse problem is well posed in the following sense. Let u_1 and u_2 be two solutions of (2) associated with the same Neumann condition ϕ on $\partial \Omega$ and to source terms F_1, F_2 of the form (1), respectively. Then, if $u_1 = u_2$ on some subset γ_* of $\partial \Omega$ that possesses an interior point, then $F_1 = F_2$. In other words, if two measured potentials associated with the same flux coincide on γ_*, then they are generated by the same source term of the form (1).

Moreover, u is harmonic in Ω_2 and Ω_1, and the Cauchy problem can be solved there, from available data on $\partial \Omega \subset \partial \Omega_2$, in order to get the value of u and $\frac{\partial u}{\partial \nu}$ on the 'inner' boundary $\partial \Omega_0 = \partial B_3$, see [40] (proposition 1 of section 2.2 below indeed allows us to transform (2) into a succession of problems in Ω_i with transmission conditions at the interfaces $\partial \Omega_i$, for $i = 0, 1$). We do not approach this important issue in the present work, and we merely consider in the following that data are available on the surface of the subdomain Ω_0 containing the source terms (brain), which is the 'inner' boundary $\partial \Omega_0$. If the constant conductivity $\sigma_0 = 1$, we are then led to the $n = 3$ situation of problems (3) and (4) below (else, divide F and ϕ there by σ_0).

More generally, the equations to come can be used to model pointwise conductivity defaults, in n-dimensional domains. Let B_n be the unit ball of $\mathbb{R}^n$, $T_n = \partial B_n$ its boundary, and ν denote the outward unit normal vector to T_n. We want to solve in B_n the inverse problem of determining a source term of the form (1), with $S_j, C_k \in B_n$, $\lambda_j \in \mathbb{R}$, $p_k \in \mathbb{R}^n$, from overdetermined boundary data

$$u_{|T_n} = g \qquad \text{and} \qquad \frac{\partial u}{\partial \nu}_{|T_n} = \phi, \tag{3}$$

of a solution u to

$$-\Delta u = F \text{ in } B_n. \tag{4}$$

Despite uniqueness holding from [29, theorem 1], let us point out that very little is known mathematically about the stability of such a problem. For the 2D case of dipolar sources, it has been studied in [21], where logarithmic stability estimates are established, assuming in addition the boundedness of the intensities and the property that poles are *well separated*. The problem is rephrased in [47], in terms of finding simple poles in the complex plane, where a sharper stability result—actually a Hölder type one—is given. Stability results in 3D situations

and for monopolar sources are contained in [53], where a Hölder-type stability result is proved from partial overdetermined data, under *a priori* assumptions of boundedness on the potentials and further on the distribution of sources. This result is improved into a Lipschitz one when complete data are available on the outer boundary. Note that, to our knowledge, there are no other available stability properties, whence no analogous results for dipolar sources.

The final issue in studying such an inverse problem is the inversion process for the recovery itself. We shall be concerned with the number of sources, their location, their intensities and moments. In [47], a least square method under constraints is proposed in order to identify dipolar sources. In [31], a variational adjoint state approach is used to approach the EEG inverse problem. The algorithm given in [23, 29] is an algebraic method based on the reciprocity gap principle, introduced in [5] for the inverse planar crack problem. The limitation of this method is that it does not apply to mixed combinations of monopolar and dipolar sources and also that we have to know *a priori* the number of sources. It was used for other operators such as the heat equation in [30] or the Helmholtz equation in [2], and successfully extended to the transient case and to homogeneous elastic bodies.

We approach here 2D situations, where $\mathbb{R}^2 \simeq \mathbb{C}$, for which we will show that the issue can be expressed as a rational or meromorphic approximation problem on the boundary T_2 with poles constrained to belong to B_2. We will see in section 2.2, see (12), that harmonic conjugation defines a complex-valued function f, depending on the boundary data (g, ϕ) on T_2, analytic in B_2, excepted at sources, whose real part coincides with the solution u to (3), (4) there. Its best meromorphic approximants, with poles in B_2, can be computed for some $L^p(T_2)$ norms; these poles are strongly related to the singularities of f that are the sources to be recovered (they even coincide for dipolar sources, but this allows us in all cases to treat monopolar and dipolar sources on an equal footing at this approximation step).

1.3. Small size inclusions

For the purpose of mine detection, mines are considered to be small with respect to the prospected area and to have a significantly higher (metal) or lower (plastic) conductivity than the surrounding soil. Taking advantage of the smallness of the inclusions, asymptotic analyses were developed in order to design reconstruction algorithms.

In the 2D case, in the presence of small inhomogeneities of size ε, the voltage potential u_ε is a solution of

$$\begin{cases} \operatorname{div}(\gamma_\varepsilon \nabla u_\varepsilon) = 0 & \text{in} \quad B_2, \\ \dfrac{\partial u_\varepsilon}{\partial \nu}\bigg|_{T_2} = \phi. \end{cases} \tag{5}$$

The conductivity γ_ε is assumed to be equal to 1 in the safe part of the domain $B_2 \setminus \cup_{j=1}^m \omega_\varepsilon^j$ while on the jth inclusion ω_ε^j, we have $\gamma_\varepsilon = k_j$, for some constant $k_j \in \mathbb{R}_+^*$. The inhomogeneities are assumed to be of the form

$$\omega_\varepsilon^j = \varepsilon \omega_j + z_j \subset B_2. \tag{6}$$

The points $z_j \in B_2$ determine the location of the imperfections whereas the domains $\omega_j \subset \mathbb{R}^2$, which describe their relative shapes, are bounded, smooth, strictly star shaped, and contain the origin 0. The parameter ε measures the common order of magnitude of the diameter of the inclusions: it is sufficiently small, so that the inclusions are distant enough from the boundary T_2.

Now, given additional measurements of the potential on the boundary: $u_{\varepsilon|T_2} = g_\varepsilon$, the inverse problem consists in recovering the inclusion parameters k_j, z_j, ω_j and ε. In mine

detection, however, as in some other applications, the information of real interest is the positions z_j of the inclusions, and it is not always necessary to reconstruct the precise value of their conductivity nor their shape.

The asymptotic expansion of the voltage potential, derived in [32], was the fundamental step in the design of an identification procedure which consists in a discrete least square minimization method. It was also used in [3] with a variationally method based on a reciprocity gap principle. The idea was to form the integral of the measured boundary data against harmonic test functions and to choose the currents so as to reduce the reconstruction problem to the inversion of some Fourier transforms. Another algorithm that makes use of the asymptotic expansion of the voltage potential has been derived in [20] which is in the spirit of the linear sampling method of [26]. For accurate reconstruction of the location of m inhomogeneities, this method requires knowledge of the subspace spanned by the first $2m$ eigenvectors of the incremental Dirichlet to Neumann data operator. A more realistic real-time algorithm based on the observation of the pattern of a simple weighted combination of a constant input current and the corresponding output voltage is proposed in [42]. This algorithm was improved in [4], using a few more measurements, based on a new asymptotic formula and the observation in both the near and the far field of the pattern of a simple weighted combination of the input currents and the output voltages. In all of these algorithms, the locations of the inclusions are found with an error of the order of the size of the inhomogeneities.

These asymptotics, stated in section 2.3, together with harmonic conjugation, provide approximation formulae for u_ε, for small ε, by (the real part of) a meromorphic function f_ε in B_2, defined on T_2 by the available boundary data (g_ε, ϕ). The poles of f_ε then coincide with the centres z_j of the inclusions to be recovered, while their residues are explicitly linked to their parameters k_j, ω_j and ε. Hence, recovering f_ε in B_2 from its boundary values on T_2, which we approach using the best meromorphic approximation there, will solve for the inverse problem of recovering the centres of the small inclusions and their conductivities k_j, assuming that their shapes ω_j and common length ε are known.

2. Expressions of the solutions in terms of rational functions

We first set up regularity properties of the solutions $u = u_2$ and u_ε to the direct Neumann problems associated with (3) and (4) for $n = 2$, and (5), which allow us to give partially explicit representations for these and for the associated complex-valued functions f and f_ε in terms of the parameters of the sources or inclusions.

2.1. Notation

We denote by $W^{1,p}(\Omega)$ the familiar Sobolev space of $L^p(\Omega)$ functions whose distributional derivatives of first order again lie in $L^p(\Omega)$, $p \in [1, \infty]$. We put $W_0^{1,p}(\Omega)$ to denote the subspace of $W^{1,p}(\Omega)$ consisting of functions whose traces on the boundary $\partial\Omega$ vanish [35, 48]. Here, $W^{-1,p}(\Omega)$ is the dual of $W_0^{1,q}(\Omega)$ with $1/p + 1/q = 1$. Let $W^{-1/2,2}(\partial\Omega)$ be the dual space of $W_0^{1/2,2}(\partial\Omega)$, the latter being most easily described as the interpolation space (of exponent 1/2) between $W_0^{1,2}(\partial\Omega)$ and $L^2(\partial\Omega)$, [44, theorem 11.6].

2.2. The case of pointwise sources

To begin, we prove a preliminary regularity result for the solution to the extended direct Neumann problem (2) which is needed in order to express it as (4) on $\Omega_0 = B_n$.

Proposition 1. *If $\phi \in W^{-1/2,2}(\partial\Omega)$ and F given by (1) are linked by*

$$-\int_{\partial\Omega} \phi \, ds = \int_{\Omega_0} F(z) \, dz = \sum_{j=1}^{m_1} \lambda_j, \tag{7}$$

then there exists a solution u to (2), Hölder continuous in $\bar{\Omega}\backslash\{S_j, C_k\}$, and unique up to an additive constant.

The above integral of the distribution F over Ω_0 is of course to be understood as the duality product $\langle F, 1 \rangle_{\Omega_0}$.

Proof. Let E_n be a fundamental solution associated with the Laplace operator $(-\Delta)$ in $\mathbb{R}^n$ [27, 38]. We introduce the function

$$v(x) = -\frac{1}{\sigma_0} E_n * F$$

which satifies $-\sigma_0 \Delta v = F$, in Ω. Because F defined by (1) is a distribution supported by $\{S_j, C_k\} \in \Omega_0$, the above function v is harmonic and smooth outside Ω_0. In particular, $v \in C^\infty(\Omega\backslash\bar{\Omega}_0)$ so that, *a fortiori*, $\nabla \cdot ((\sigma - \sigma_0)\nabla v) \in W^{-1,p}(\Omega)$ for all p. If we consider $w = u - v$, we get

$$\begin{cases} -\nabla \cdot (\sigma \nabla w) = \nabla \cdot ((\sigma - \sigma_0)\nabla v) \text{ in } \Omega \\ \sigma \dfrac{\partial w}{\partial \nu}_{|\partial\Omega} = \phi - \sigma \dfrac{\partial v}{\partial \nu}_{|\partial\Omega} . \end{cases} \tag{8}$$

If $\phi \in W^{-1/2,2}(\partial\Omega)$, the compatibility condition

$$\int_{\partial\Omega} \left(\phi - \sigma \frac{\partial v}{\partial \nu} \right) ds = \int_{\Omega} \nabla \cdot ((\sigma - \sigma_0)\nabla v) \, dz,$$

which, from Ostrogradski's formula and Gauss's theorem, together with the above definition of v, simply becomes (7) and is sufficient to ensure the existence of a weak (or generalized) solution $w \in W^{1,2}(\Omega)$ to the direct Neumann problem (8). This follows from classical existence results concerning strictly elliptic second-order problems in bounded smooth domains, see [27, II.8.4, proposition 10].

For $n \geqslant 2$ however, Sobolev's imbedding theorems do not ensure the continuity of functions in $W^{1,2}(\Omega)$ which indeed contains discontinuous elements. However, the De Giorgi–Nash theorem asserts that a solution $w \in W^{1,2}(\Omega)$ to the above divergence form (8) is in fact Hölder continuous in $\bar{\Omega}$, see [27, II.8.3, proposition 6], [34, theorem 8.22]. In particular, w is continuous through the different layers. This shows that a solution u to (2) is Hölder continuous in $\bar{\Omega}\backslash\{S_j, C_k\}$, and is unique up to an additive constant. $\qquad\square$

We now see that (2) can be rewritten as

$$-\Delta u = 0 \text{ in } \Omega_i, \qquad i = 1, 2, \qquad -\Delta u = F \quad \text{in} \quad \Omega_0 = B_n,$$

which contains (4), whence, thanks to proposition 1, u is smooth enough for the following transmission conditions to hold, in addition to those acting on the outer boundary $\partial\Omega = \partial\Omega_2$:

$$u^+ = u^- \qquad \text{and} \qquad \sigma_i \frac{\partial u^+}{\partial \nu} = \sigma_{i-1} \frac{\partial u^-}{\partial \nu} \quad \text{on } \partial\Omega_i \cap \partial\Omega_{i-1}, \qquad i = 1, 2,$$

where superscripts '+' and '−' indicate the limiting values as we approach $\partial\Omega_i \cap \partial\Omega_{i-1}$ from Ω_i (outside) and Ω_{i-1} (inside), respectively. This allows us to express the boundary condition on $\partial\Omega_0 = T_n$ as (3). We thus turn to Laplace equation (4), for which the following corollary of proposition 1, see also [27, II.8.3, proposition 6], holds.

Corollary 1. *Assume $\phi \in W^{-1/2,2}(T_n)$. If the compatibility condition*

$$-\int_{T_n} \phi \, ds = \sum_{j=1}^{m_1} \lambda_j = \int_{B_n} F(z) \, dz \tag{9}$$

holds, the solution to the direct Neumann problem associated with (4) is unique up to an additive constant and Hölder continuous in $\overline{B}_n \backslash \{S_j, C_k\}$.

Assume now that $n = 2$.

Proposition 2. *There exists a function $\mathcal{A}$ analytic in B_2 such that, if we define*

$$f(z) = \mathcal{A}(z) - \sum_{j=1}^{m_1} \frac{\lambda_j}{2\pi} \log(z - S_j) - \sum_{k=1}^{m_2} \frac{p_k}{2\pi(z - C_k)}, \tag{10}$$

then

$$u_2(z) = \mathrm{Re}(f(z)), \qquad z \in B_2 \backslash \{S_j, C_k\}.$$

Moreover, if

$$\int_{T_2} \phi \, ds = 0, \tag{11}$$

then f is given on T_2 (up to an additive constant) by

$$f(z) = g(z) + \mathrm{i} \int_{\xi_0}^{z} \phi(\xi) \, ds(\xi), \tag{12}$$

for every $z \in T_2$, where $\xi_0 \in T_2$ is fixed once and for all.

Proof. Any solution $u = u_n$ to (4) can be written as

$$u_n(z) = h_n(z) + \int_{B_n} E_n(z, x) F(x) \, dx,$$

for $z \in B_n \backslash \{S_j, C_k\}$, where h_n is a harmonic function in B_n [27, 38]. The radial fundamental solution of $-\Delta$ in $\mathbb{R}^2 \backslash \{0\}$, $E_2(z, x) = E_2(z - x)$ is given by

$$E_2(z) = -\frac{1}{2\pi} \log |z|, \tag{13}$$

so we get the following expressions for the solution to (4) *in the case $n = 2$ to which we stick in the following*:

$$u_2(z) = h_2(z) - \sum_{j=1}^{m_1} \frac{\lambda_j}{2\pi} \log |z - S_j| - \sum_{k=1}^{m_2} \frac{p_k \cdot (z - C_k)}{2\pi |z - C_k|^2}. \tag{14}$$

We now turn to the complex framework, where the vector $z = {}^t(z_1, z_2) \in \mathbb{R}^2$ is identified with the complex number $z = z_1 + \mathrm{i} z_2 \in \mathbb{C}$, for simplicity. With this notation, (14) becomes

$$u_2(z) = \mathrm{Re}(f(z)), \qquad z \in B_2 \backslash \{S_j, C_k\},$$

with f defined by (10), where $\mathcal{A}$ is a function analytic in B_2 such that $h_2 = \mathrm{Re}\,\mathcal{A}$. The function f is thus analytic on an annulus in B_2 surrounded by T_2 that does not contain any source $\{S_j, C_k\}$. Hence, thanks to Cauchy–Riemann equations, it holds from the boundary conditions (3) and (11) that f is given on T_2 up to an additive constant by (12). $\square$

The inverse source problem in B_2 can then be formulated as that of locating the singularities of the function f given by (10) from its values on the boundary T_2 of B_2, available from (12) from Cauchy data g, ϕ (3).

In the case where there are no sources in B_2, i.e $m_1 = m_2 = 0$, the function u_2 is the real part of the analytic function $\mathcal{A} = f$ which is known on T_2. This provides the basis of a test to establish the presence of sources in the domain. Indeed, some distance on T_2 between f and the set of boundary values of analytic functions in B_2 can be constructively computed, at least for quadratic and uniform norms [1, 7, 13, 50].

This is where Hardy spaces H^p come in. If this distance is strictly positive (not too small, in practice) f does necessarily possess singularities in B_2 and we are led to the determination of the number of sources, their positions and their moments. This issue can be approached through the study of the behaviour of the poles of rational or meromorphic approximants on T_2.

2.3. The case of small inclusions

When the number m and the size ε of the inclusions are small enough, the solution u_ε to (5) is close to the background potential u which is a solution to the homogeneous problem

$$\begin{cases} \Delta u = 0 \text{ in } B_2, \\ \dfrac{\partial u}{\partial \nu}\Big|_{T_2} = \phi, \end{cases} \tag{15}$$

provided that both satisfy the same normalization condition

$$\int_{T_2} u \, ds = \int_{T_2} u_\varepsilon \, ds = 0, \tag{16}$$

which ensures uniqueness. Observe that the existence of solutions u and u_ε to (16) and (5) is guaranteed by the compatibility condition (11).

Also, if $\phi \in W^{-1/2,2}(T_2)$, then $u, u_\varepsilon \in W^{1,2}(B_2)$ and are Hölder continuous in $\bar{\Omega}$; this follows, as in proposition 1, from the De Giorgi–Nash theorem [27, II.8.3, proposition 6], [34, theorem 8.22].

Let E_2 be the fundamental solution of the 2D Laplace operator given by (13), and $\dfrac{\partial E_2}{\partial \nu_x}(x, z) = \nabla_x E_2(x, z) \cdot \nu$.

Theorem 1 ([18], [32]). *When B_2 contains m well-separated circular inclusions, $\omega_\varepsilon^i = z_i + \varepsilon B_2$, with conductivity k_i, then for $z \in T_2$*

$$u_\varepsilon(z) - u(z) + 2\int_{T_2} (u_\varepsilon(x) - u(x)) \frac{\partial E_2}{\partial \nu_x}(x, z) \, ds(x)$$

$$= -\varepsilon^2 \frac{1}{\pi} \sum_{i=1}^{m} \frac{z - z_i}{|z - z_i|^2} \cdot A_i \nabla u(z_i) + O(\varepsilon^{5/2}). \tag{17}$$

The polarization tensor $A_i = \left(a_{jl}^{(i)}\right)$ corresponding to the ith inhomogeneity is given by

$$a_{jl}^{(i)} = \pi \frac{1 - k_i}{1 + k_i} \delta_{jl}, \qquad j, l = 1, 2. \tag{18}$$

where δ_{jl} denotes the Kronecker symbol. For a domain with two close-to-touching circular inclusions of common size ε and conductivity k, separated by $2\delta\varepsilon$, $\delta \geqslant 0$, we have for $z \in T_2$:

$$u_\varepsilon(z) - u(z) + 2\int_{T_2} (u_\varepsilon(x) - u(x)) \frac{\partial E_2}{\partial \nu_x}(x, z) \, ds(x) = -\varepsilon^2 \frac{1}{\pi} \frac{z - z_0}{|z - z_0|^2} \cdot A \nabla u(z_0) + O(\varepsilon^3) \tag{19}$$

where z_0 is a point in the convex hull of the union of the two inclusions and $A = (a_{jl})$ is equal to

$$a_{jl} = \begin{cases} 16a^2\pi \sum_{n \geqslant 1} n \dfrac{\rho^{2n}}{\Lambda + (-1)^j \rho^{2n}} \delta_{jl}, & \text{if } \delta \neq 0, \\[2ex] (-1)^{j+1} 4\pi \sum_{n \geqslant 1} \dfrac{(-1)^{(j+1)n}}{\Lambda^n n^2} \delta_{jl}, & \text{if } \delta = 0, \end{cases} \qquad j, l = 1, 2, \qquad (20)$$

where $\Lambda = \frac{k+1}{k-1}, a = \sqrt{\delta(2+\delta)}, \rho = \frac{a-\delta}{a+\delta}$.

Therefore, u is the first term in the asymptotic expansion of u_ε, as $\varepsilon \to 0$. The correction of order two for this expansion was derived in [32] for a domain with a finite number of small well-separated inclusions and in [18] for two small close-to-touching inclusions, in terms of their properties (location, shape and conductivity), through the so-called polarization tensors.

Remark 1. Expression (17) is still valid for more general configurations [32, theorem 2]. In fact, consider an open bounded smooth domain Ω in $\mathbb{R}^n$, $n \geqslant 2$, of conductivity 1. Assume that Ω contains m well-separated inclusions $\omega_\varepsilon^i = z_i + \varepsilon\omega_i$, where $\omega_i \subset \mathbb{R}^n$ is a strictly star-shaped, bounded, smooth domain containing the origin, with conductivity k_i, then formula (17) holds true for every $z \in \partial\Omega$. In this case, the polarization tensor $A_i = \left(a_{jl}^{(i)}\right)$, associated with ω_i, is a symmetric matrix (see [51]) given by

$$a_{jl}^{(i)} = \frac{1 - k_i}{k_i} \left(|\omega_i| \delta_{jl} + \int_{\partial\omega_i} \frac{\partial \phi_j^{(i)+}}{\partial \nu^{(i)}}(y) y_l \, ds(y) \right), \qquad j, l = 1, \ldots, n, \qquad (21)$$

where $|\omega_i|$ denotes the Lebesgue measure of the domain ω_i, $\nu_j^{(i)}$ the jth component of the outward unit normal vector to $\partial\omega_i$, and $\phi_j^{(i)}$ is the solution of the following free space Laplace equation:

$$\begin{cases} \Delta\phi_j^{(i)} = 0 \text{ in } \omega_i, \qquad \Delta\phi_j^{(i)} = 0 \text{ in } \mathbb{R}^2 \backslash \omega_i, \\[1ex] \phi_j^{(i)} \text{ is continuous across } \partial\omega_i \text{ and } \lim_{|y| \to \infty} \phi_j^{(i)}(y) = 0, \\[1ex] \dfrac{1}{k_i} \dfrac{\partial\phi_j^{(i)+}}{\partial\nu^{(i)}} - \dfrac{\partial\phi_j^{(i)-}}{\partial\nu^{(i)}} = \dfrac{1 - k_i}{k_i} \nu_j^{(i)} \text{ on } \partial\omega_i, \end{cases}$$

where superscripts '+' and '−' indicate the limiting values as we approach $\partial\omega_i$ from outside and inside ω_i, respectively.

Remark 2. If the inclusions are 'well separated' and of smooth shape, the gradient of the potential u_ε (which represents the stress in this case) is uniformly bounded. Such a picture could deteriorate when some inclusions get close-to-touch, forming narrow channels where currents could concentrate. For finite and strictly positive conductivity, it has been shown in [19, 43] that, when Ω and the inclusions are bounded domains with $C^{1,\alpha}$ boundaries, $0 < \alpha < 1$, the function u_ε is in $W^{1,\infty}(\Omega)$. The bound on the stress depends on k_j, the size and the shape of the inhomogeneities (on the $C^{1,\alpha}$ modulus of the total boundary of all the subdomains). This result is optimal in terms of global regularity, since ∇u_ε is generically discontinuous at the interfaces between the inclusions and the background domain.

Proposition 3. *There exists a unique function f_ε meromorphic in B_2 with poles at $\{z_i\}$ such that*

$$u_\varepsilon(z) = \text{Re}(f_\varepsilon(z)), \qquad z \in T_2,$$

where f_ε admits expression (23) or (24), Moreover, if ϕ satisfies (11), then f_ε is given on T_2 by

$$f_\varepsilon(z) = g_\varepsilon(z) + \mathrm{i} \int_{\xi_0}^z \phi(\xi)\, \mathrm{d}s(\xi), \tag{22}$$

for every $z \in T_2$ and some fixed $\xi_0 \in T_2$.

Proof. Thanks to expressions (17) and (19), it holds that $u_\varepsilon = \mathrm{Re}\, f_\varepsilon$ on T_2, for f_ε defined in $B_2 \backslash \{z_i\}$ by

$$f_\varepsilon(z) = \mathcal{C}_\varepsilon(z) - \varepsilon^2 \frac{1}{\pi} \sum_{i=1}^m \frac{A_i \nabla u(z_i)}{z - z_i} + O(\varepsilon^{5/2}), \tag{23}$$

in the case of m separate inclusions or, for two close inclusions, by

$$f_\varepsilon(z) = \mathcal{C}_\varepsilon(z) - \varepsilon^2 \frac{1}{\pi} \frac{A \nabla u(z_0)}{z - z_0} + O(\varepsilon^3), \tag{24}$$

for some function $\mathcal{C}_\varepsilon$ analytic inside B_2 such that, on T_2,

$$\mathrm{Re}\, \mathcal{C}_\varepsilon(z) = u(z) + 2 \int_{T_2} (u(x) - u_\varepsilon(x)) \frac{\partial E_2}{\partial \nu_x}(x, z)\, \mathrm{d}s(x).$$

Thanks again to Cauchy–Riemann equations, and from the boundary conditions, f_ε is given on T_2 by (22). $\qquad \square$

We can then approximately reduce the inverse conductivity problem for small size inclusions to that of locating the singularities of a meromorphic function f_ε, whose real part is equal to u_ε, from knowledge of it on the boundary T_2. From (23) and (24), we indeed see that the localization of the inclusions in B_2 can still be expressed as finding the poles of a function f_ε from knowledge of it (22) on the boundary T_2, given by that of the boundary data g_ε, ϕ; the associated residues then give the unknown conductivities.

3. Hardy classes and best meromorphic approximation

We denote by H^2 the Hardy space of analytic functions in the unit disc B_2 of the complex plane $\mathbb{C}$ whose L^2 norms on circles of radius less then 1 are bounded. It (or its trace on T_2) can alternatively and equivalently be defined as the subspace of $L^2(T_2)$ of functions with vanishing Fourier coefficients of negative index. Let $\bar{H}_0^2$ be its orthogonal complement in $L^2(T_2)$, which consists in functions analytic outside B_2, vanishing at ∞, and whose L^2 norms on circles of radius greater than 1 are bounded [28, 33, 39]. From Parseval's equality:

$$H^2 = \left\{ \sum_{n \geq 0} a_n z^n, z \in B_2, \sum_{n \geq 0} |a_n|^2 < \infty \right\},$$

$$\bar{H}_0^2 = \left\{ \sum_{n < 0} a_n z^n, z \in B_2, \sum_{n < 0} |a_n|^2 < \infty \right\}.$$

Lemma 1. *Equations (10), (23) and (24) define functions $f - \mathcal{A}$ and $f_\varepsilon - \mathcal{C}_\varepsilon$ that belong to $\bar{H}_0^2$.*

Proof. Consider the first expression (10) for the function f. Because f is given on T_2 by (12), proposition 1 ensures that f belongs to $L^2(T_2)$ as soon as the boundary data $\phi \in W^{-1/2,2}(T_2)$. We can thus recover its Fourier coefficients, hence those of its antianalytic part $f - \mathcal{A}$ which belongs to $\bar{H}_0^2$. Indeed, the compatibility condition (9) together with (11) imply that[5]

---
[5] If $\sum_{j=1}^{m_1} \lambda_j \neq 0$, one can use the trick of adding an fictitious source with a moment $\lambda_0 = -\sum_{j=1}^{m_1} \lambda_j$.

$$\sum_{j=1}^{m_1} \lambda_j = 0, \tag{25}$$

whence $f - \mathcal{A}$ vanishes at infinity:

$$f(z) - \mathcal{A}(z) = \sum_{j=1}^{m_1} \frac{\lambda_j}{2\pi} \log \frac{z - S_j}{z - b} + \sum_{k=1}^{m_2} \frac{p_k}{2\pi(z - C_k)}, \tag{26}$$

for some arbitrary $b \in B_2$, because of (25). Since $h = f - \mathcal{A}$ is also analytic outside $\mathbb{D}$ and bounded in $L^2(T_2)$, it finally belongs to $\bar{H}_0^2$.

Concerning expressions (23) and (24), one analogously proves that $f_\varepsilon - \mathcal{C}_\varepsilon \in \bar{H}_0^2$, for $\phi \in W^{-1,2}(T_2)$, see section 2.3. □

This is how meromorphic approximation on the boundary comes in, for the recovery of these singularities in B_2 from available data on T_2. Note that the singularities of the functions to be approximated are either poles or essential singularities (log) for f (or $f - \mathcal{A}$), depending on whether $m_1 = 0$ or not, or close to the poles of some rational function for f_ε (or $f_\varepsilon - \mathcal{C}_\varepsilon$).

The next three sections consist in a survey of existing and referenced results about meromorphic approximation with constrained poles. We choose to stick to a somewhat informal presentation that we expect to briefly present the theoretical and constructive bases of the numerical schemes used in section 4.

3.1. Rational L^2 approximation

Let $R_n \subset \bar{H}_0^2$ be the set of rational functions with at most n poles in B_2, none on T_2. For functions $h \in L^2(T_2)$, the issue of the best L^2 meromorphic approximation to h with less than n poles in B_2 amounts to finding $\psi_n \in H^2 + R_n$ such that

$$\|h - \psi_n\|_{L^2(T_2)} = \min_{\psi \in H^2 + R_n} \|h - \psi\|_{L^2(T_2)}.$$

It can be expressed in terms of the best rational approximation as follows. Let P_{H^2} denote the orthogonal projection from $L^2(T_2)$ onto H^2 and $P_{\bar{H}_0^2}$ denote the one from $L^2(T_2)$ onto $\bar{H}_0^2$. Put $h_- = P_{\bar{H}_0^2} h$.

Now, being given a function $h_- \in \bar{H}_0^2$, one can look for its best L^2 rational approximation of degree less than n in $\bar{H}_0^2$: find polynomials π_n, q_n, with $\deg q_n \leqslant n$, such that $\pi_n/q_n \in \bar{H}_0^2$ (this forces $\deg \pi_n < \deg q_n$), that minimizes $\|h_- - p/q\|_{L^2(T_2)}$ among such functions, see [13]:

$$\left\| h_- - \frac{\pi_n}{q_n} \right\|_{L^2(T_2)} = \min_{\deg p < \deg q = n} \left\| h_- - \frac{p}{q} \right\|_{L^2(T_2)}.$$

It then holds that $\psi_n = P_{H^2} h + \pi_n/q_n$.

The existence of such a minimum is established in [6]. In fact, q_n will have degree n, except if h_- is already a rational $\bar{H}_0^2$ function of degree strictly less than n (normality property) [13].

As to uniqueness of the best rational approximant, it is known to be true for an open and dense subset of $\bar{H}_0^2$. Whenever h_- itself is a rational function of degree n in $\bar{H}_0^2$, the unique minimum at order n is h itself, a consequence of the consistency property from [12] (which is to the effect that h_- is the unique critical point of the criterion). In general, however, local minima do exist.

Concerning constructive aspects, algorithms to generate local minima can be obtained using Schur parametrization which induces a map on the manifold consisting in rational

$\bar{H}_0^2$ functions of given degree (possibly high, in order to model or closely approximate the given function, and equal to n for the solution) and of uniform norm equal to 1 on T_2 [46]. Computing the gradient and the Hessian of the criterion with this parametrization produces an efficient resolution scheme, see section 4.

3.2. Best uniform meromorphic approximation

The following extremal issue of best uniform meromorphic approximation on T_2 is the so-called Adamjan–Arov–Krein (AAK) problem [1, 50, 54]. Being given some function $h \in L^\infty(T_2)$, find a best approximant ψ_n to h in $L^\infty(T_2)$-norm among the set $H^\infty + R_n$ of functions meromorphic with at most n poles in B_2 and bounded near T_2:

$$\min_{\psi \in H^\infty + R_n} \|h - \psi\|_{L^\infty(T_2)} = \|h - \psi_n\|_{L^\infty(T_2)}. \tag{27}$$

Although (27) admits solutions for every $h \in L^\infty(T_2)$, the uniqueness is only ensured whenever $h \in H^\infty + C(T_2)$, that is when $h_- \in C(T_2)$.

In this case, the Hankel operator $\mathcal{H}_h$ of symbol h defined on H^2 by

$$\mathcal{H}_h \psi = P_{\bar{H}_0^2}(h\psi), \qquad \forall \psi \in H^2$$

is compact [54]. Note that $\mathcal{H}_h = \mathcal{H}_{h_-}$, since the H^∞ part of the symbol. The best meromorphic approximant with at most n poles in B_2, also called the AAK approximant of order n, to a function $h \in H^\infty + C(T_2)$ is given by

$$\psi_n = h - \frac{\mathcal{H}_h v_n}{v_n}, \tag{28}$$

for the first element v_n of the $(n+1)$th Schmidt pair of $\mathcal{H}_h$, see [50, 54]. Moreover, the error is circular: $|h - \psi_n| = \sigma_n$ a.e. on T_2, σ_n being the $(n+1)$th singular value of $\mathcal{H}_h$. Since $\mathcal{H}_h$ is compact, we can equivalently define (σ_n^2, v_n) as the eigenvalues and eigenvectors of the self-adjoint compact operator $\mathcal{H}_h^* \mathcal{H}_h$:

$$\mathcal{H}_h^* \mathcal{H}_h v_n = \sigma_n^2 v_n.$$

For meromorphic symbols $h \in H^\infty + R_N$, that is $h_- \in R_N$, $\mathcal{H}_h = \mathcal{H}_{h_-}$ has finite rank and the above procedure can be made constructive by building its singular values decomposition. Continuity properties from [49] show that it remains generically effective (robust) when h_- is Hölder smooth on T_2 and can be approximated there by rationals in the Hölder norm.

This uniform approximation procedure may be used either directly as an alternative to the quadratic one explained in section 3.1 or in order to initialize it at the target degree. We mainly use it in this second way, since the L^2 scheme carries additional robustness and smoothness properties, with respect to noise, see section 4.

3.3. Behaviour of poles

When the function h to be approximated is already meromorphic with poles in B_2, that is when the antianalytic part $h_- = P_{\bar{H}_0^2} h$ belongs to R_m or is already rational of degree m, the best rational approximant π_n/q_n of degree n will coincide with h_- and provide 0 as error value, as soon as $n \geqslant m$. This occurs in the case of dipolar sources where $m_1 = 0$, since then $f - \mathcal{A} \in R_{m_2}$ from (10), and is 'almost' true concerning small inclusions, since $f_\varepsilon - \mathcal{C}_\varepsilon$ is close to R_m from (23) or (24), with $m = 1$. This allows us to recover the number m of poles (even in cases where it is high enough), together with their locations and residues. Indeed, if $n > m$, π_n/q_n possesses n poles, among which $n - m$ have a residue equal to zero. The same phenomenon occurs with the AAK approximation.

When the function h to be approximated is not meromorphic, this is no longer true, since the latter no longer belongs to the approximating class. However, when h has branchpoints as

singularities, such as log-type ones, for example as in (10) above, some weaker information is still available about their location from the behaviour of the poles of best approximants.

Concerning pointwise sources, in the purely monopolar case where $m_1 = 2$ and $m_2 = 0$ and where $\lambda_1 = -\lambda_2$, from the compatibility condition (25), the antianalytic part $h_- = f - \mathcal{A}$ of the function f defined by (10) can be written as

$$h_-(z) = -\lambda_2 \int_\gamma \frac{\mathrm{d}\xi}{z - \xi},$$

for any curve γ joining S_1 and S_2 in B_2. It can then be proved as a consequence of potential theory, see [10, 11, 14, 41, 45], that the counting measure of the poles of the best L^2 or L^∞ rational approximant (namely the probability measure having equal mass at each of these poles) converges in the weak-$*$ sense when n goes to infinity to the Green equilibrium distribution of the circle orthogonal to T_2 joining S_1 and S_2 in B_2.

Because equilibrium distributions charge the endpoints, S_1 and S_2 will be accumulation points of the poles and should therefore be detected.

Note that the arc of the circle orthogonal to T_2 joining S_1 and S_2 in B_2 is the hyperbolic geodesic arc between these points, which is the reason why it appears in this context[6].

Further, it is conjectured that this holds for more than two points, namely the counting measure of the poles of the best approximants to the singular part of (10)—more generally to functions belonging to a class of Cauchy integrals on some contour joining the m_2 points S_j—converges in the weak-$*$ sense when n goes to infinity to the equilibrium distribution on the contour $\mathcal{J}$ connecting the S_j that minimizes the capacity of the condensor $(T_2, \mathcal{J})$. This is illustrated by the numerical experiments of sections 4.1.2 and 4.1.3.

Hence, the behaviour of the best meromorphic approximants gives weaker information about the location sources in the monopolar case than in the dipolar one, although the above convergence result indicates that the efficiency of the best approximation schemes in order to recover such singularities depends strongly on the number of numerically computed poles, since they only accumulate towards the S_j. This property however allows us at least to get a first estimation of the monopolar sources location and possibly initialize existing more appropriate but expensive localization procedures. See also [8] where this property is used for cracks recovery and [16] where the AAK approximation is used in order to build extensions of partial boundary data for solving inverse problems for cracks.

4. Numerical experiments

They are produced by the software *Rarl2*[7] which uses the procedure described in section 3.1, relying on Schur parameters, in order to compute the best rational $\bar{H}_0^2$ approximants π_n/q_n of given degree n to the function $h \in \bar{H}_0^2$. This software also performs the AAK approximation, as described in section 3.2, using singular value decompositions together with state space representations.

4.1. Pointwise sources

We first solve the direct Neumann problem (3), (4) for $n = 2$. The domain B_2 is meshed using P1 finite elements from the Matlab toolkit *PDEtool*. The boundary T_2 is discretized with 512 points. We compute the values at these points of the potential u_2 associated with the following boundary currents on T_2: $\phi_1(\theta) = \cos^2\theta \sin\theta - 1/2$, $\phi_2(\theta) = \cos\theta$ and the

---

[6] More can be said, namely the sum of the angles under which the poles see this arc of circle is bounded by an absolute constant, see [41, 45].

[7] Developed jointly at INRIA (Miaou team) and Ecole des Mines de Paris (CMA) using Matlab 6.
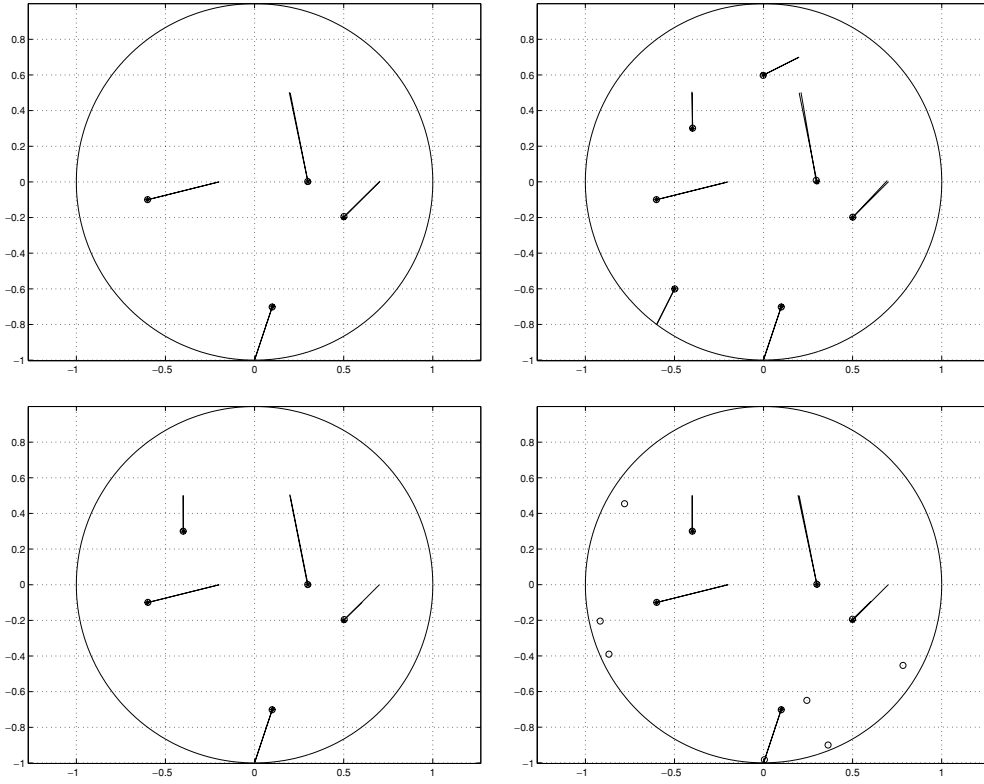
Figure 1. $m_2 = n = 4$; $m_2 = n = 7$; $m_2 = 5, n = 5, 12$.

piecewise continuous flux $\phi_3(\theta)$ equal to 1 when $\theta \in [0, \pi/2[$, to -1 if $\theta \in [\pi, 3\pi/2[$ and to 0 otherwise. We then build from (12) pointwise values on T_2 of a function f whose expression is given by (10) and the associated Fourier series (usually with 500 coefficients). Its antianalytic part $h_- = f - \mathcal{A}$ is then obtained by keeping the Fourier coefficients of negative indices (250 coefficients).

In the following figures, the original sources are represented by (small) $*$, the recovered poles by the $\circ$ (which are often superposed on the $*$, which makes them look like single black circles), while the lines are the moments for both functions (symbolized by a dot when equal to 0 or sufficiently small).

4.1.1. Dipolar sources, $m_1 = 0$. In that case, the function $h_- = f - \mathcal{A}$ to be approximated is already rational of degree m_2. Whenever $n = m_2$, the best L^2 rational approximant π_n/q_n of degree n as well as the AAK approximant ψ_n will coincide with h_- itself and provide a vanishing, numerically small, error value, as explained in section 3.3. This scheme also allows us to recover the number m_2 of dipoles (even in cases where it is high enough), their locations C_k and moments p_k (given by residues at poles C_k), $k = 1, \ldots, m_2$, since, if $n > m_2$, π_n/q_n and ψ_n possess n poles in B_2, among which $n - m_2$ have a moment (or residue) close to zero. Figures 1 to 3 illustrate how the computation of the poles of best L^2 rational approximants to h_- on T_2 (antianalytic part of boundary data) allows us to recover the dipoles. Only the last plot in figure 3 concerns the AAK approximation. Except in figure 2, we have $\phi = \phi_1$.
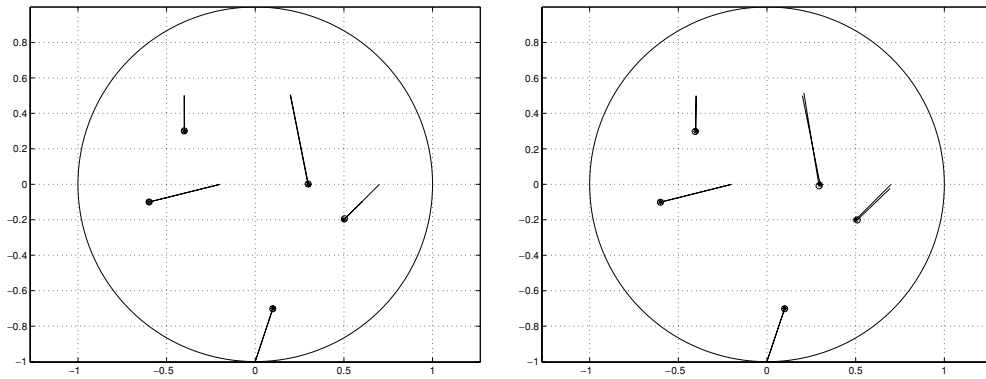
Figure 2. $m_2 = 5$; flux ϕ_2, ϕ_3.
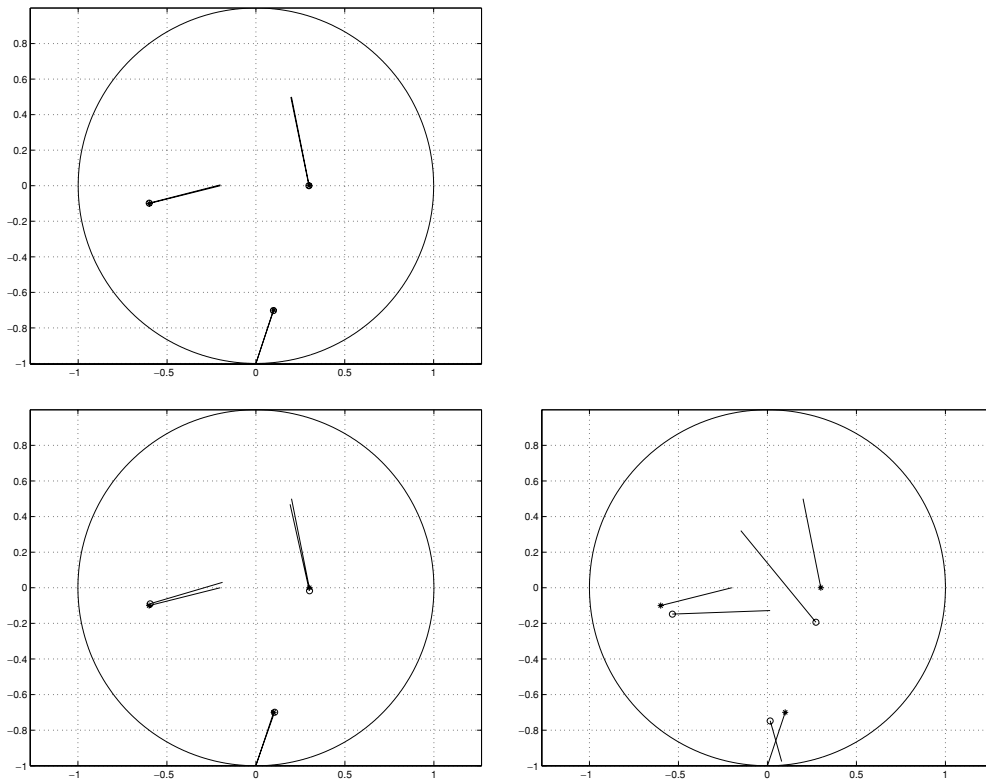

Figure 3. $m_2 = 3$; noise 1% using L^2; noise 10% using L^2 and AAK.

In figure 1, we see that this method is efficient even for a relatively large number of dipoles and that it also allows us to find the number m_2 of dipoles. In fact, if m_2 is unknown, we increase the degree n of the rational approximant until the appearance of a pole with zero residue. The number m_2 of dipoles is then equal to the number of poles with nonzero residue (see the last plot).

An analysis of the l^2 error in the location of the recovered dipoles confirms the accuracy of our method, although the error increases with the number of sources. In fact, it varies
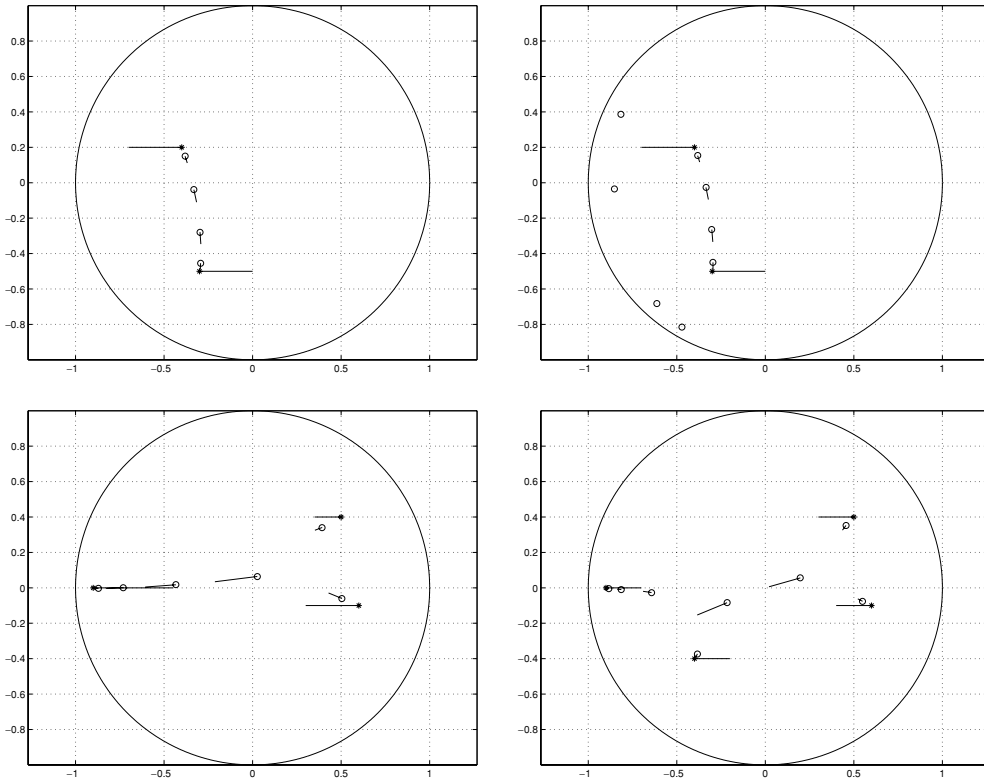
Figure 4. $m_1 = 2, n = 4, 8; m_1 = 3, n = 6; m_1 = 4, n = 8$.

from 3×10^{-3} for a configuration with $m_2 = 2$ to 6×10^{-3} and 10^{-2} for $m_2 = 5, 7$, respectively.

The same remark is valid when we study the relative l^2 error for the moments of the sources. The error is equal to 2×10^{-4} for $m_2 = 2$ dipoles, to 9×10^{-3} for $m_2 = 5$, and to 3×10^{-2} for $m_2 = 7$, in figure 1.

We have also tested this identification process with respect to different fluxes. Figure 2 is obtained using the fluxes ϕ_2 and ϕ_3. All these fluxes allow us to identify the sources but, for these configurations, the results associated with the fluxes ϕ_1 and ϕ_2 are more accurate than those computed using the piecewise constant flux ϕ_3, which is due to the error arising from the truncation of the Fourier series. In fact, for the test with five dipoles in figure 2, the relative l^2 error for the moments is equal to 9×10^{-3} for the two first fluxes and to 6×10^{-2} for ϕ_3, whereas the errors in the locations are respectively 6×10^{-3} and 10^{-2}.

We now consider the robustness properties of our identification processes. We obtain good results for perturbed data with an additive random noise whose amplitude is taken to be equal to $x\%$ of the uniform norm of (the available pointwise values of) u_2 on T_2.

Our choice of the rational L^2 approximation instead of the best uniform meromorphic one is motivated by the fact that the first one is much more robust than the second approximation, as discussed in section 3.2. Although the robustness of both algorithms deteriorates as the number of sources increases, the L^2 method is strongly stable when the domain contains only a small number of dipolar sources. This is already shown in figure 3, where an AAK procedure is run instead of the L^2 one, in the last plot.
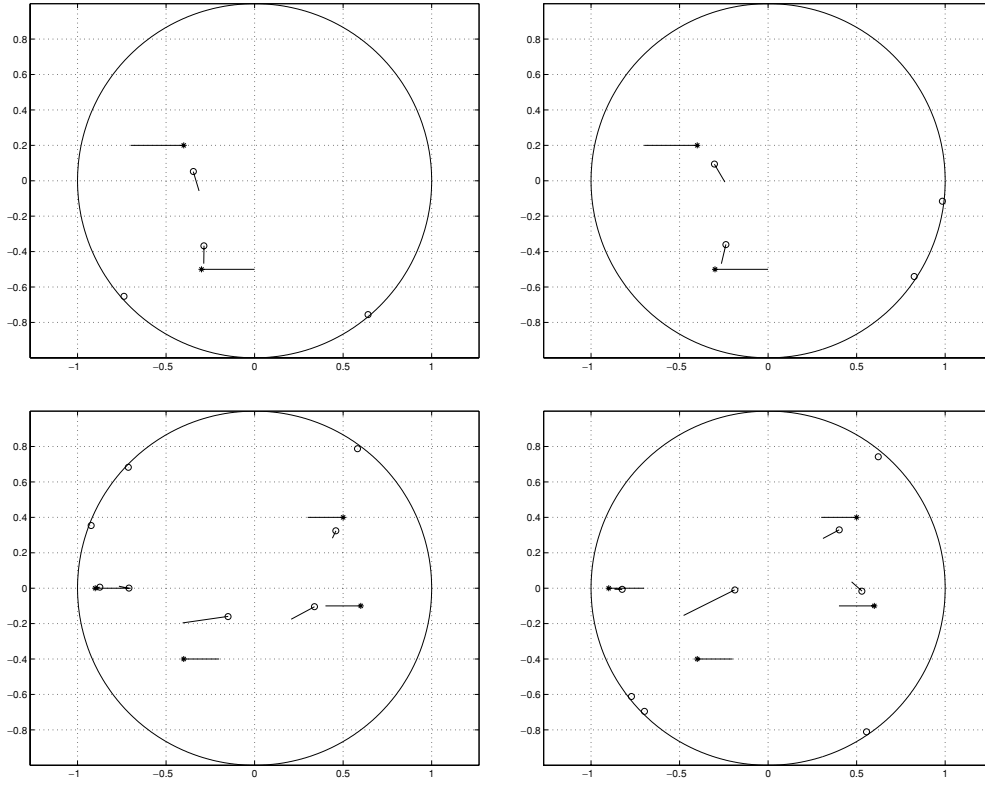
Figure 5. $m_1 = 2, n = 4$; $m_1 = 4, n = 8$; noise 1% and 5%.

4.1.2. Monopolar sources, $m_2 = 0$. We follow the same steps as for the identification of dipolar sources in 4.1.1. In this case, the function $h_- = f - \mathcal{A}$ to be approximated is no longer rational but has branchpoints. The behaviour of the poles of the best approximants to h_- is described in section 3.3 and confirmed by the numerical tests.

In fact, we clearly see in figure 4 how the poles of the best approximant accumulate towards $\{S_j\}_{1 \leqslant j \leqslant m_1}$, on the contour γ joining the S_j which minimizes the capacity of the condensor (T_2, γ).

For noisy data, we lose a part of the information, since we have fewer poles on the contour joining the sources, but we still get an idea about their behaviour, see figure 5.

Assuming that the sources (S_j), $1 \leqslant j \leqslant m_1$ are determined, the following relations allow us to compute the associated moments (λ_j), if (25) holds. Let w be an analytic function in B_2 and let $a \in B_2$ such that the lines between a and S_j are two by two distinct. From (26),

$$\int_{T_2} w(z) f(z) \, dz = \int_{T_2} w(z) h_-(z) \, dz$$

$$= \int_{T_2} w(z) \sum_{j=1}^{m_1} \frac{\lambda_j}{2\pi} \log \frac{z-a}{z-S_j} \, dz = \int_{\cup \Gamma_j} w(z) \sum_{j=1}^{m_1} \frac{\lambda_j}{2\pi} \log \frac{z-a}{z-S_j} \, dz$$

where $\cup_{j=1}^{m_1} \Gamma_j$ is a closed path surrounding the segments $[aS_j]$, $j = 1, \ldots, m_1$, from Cauchy's theorem. The last integral is independent of the choice of the point a and the paths Γ_j; assuming that the lines $(0S_j)$ are two by two distinct, we can thus choose $a = 0$, the origin, and a closed
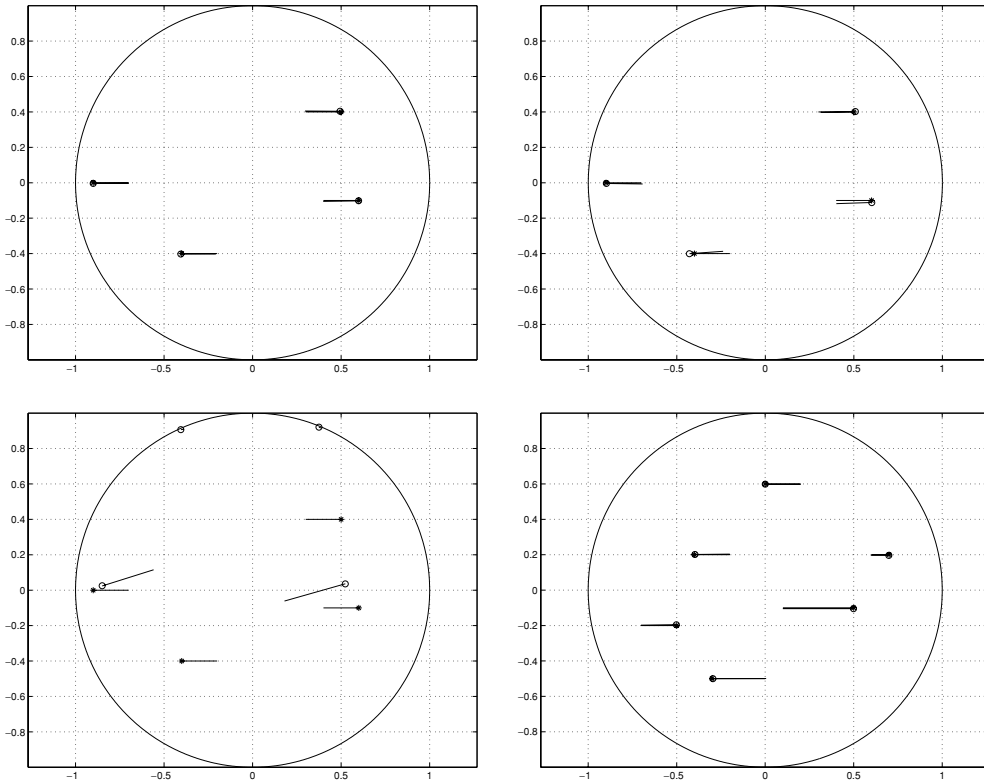
Figure 6. $m_1 = n = 4$, noise 0%, 1%, 5%; $m_1 = n = 6$.

path $\cup_{j=1}^{m_1} \Gamma_j$ surrounding $\cup_{j=1}^{m_1} [0 S_j]$. So, because the determinations of the log term above differ by $2i\pi$ on both sides of $[0 S_j]$, we obtain that

$$\int_{T_2} w(z) f(z) \, \mathrm{d}z = \sum_{j=1}^{m_1} i\lambda_j \int_{\Gamma_j} w(z) \, \mathrm{d}z = \sum_{j=1}^{m_1} i\lambda_j S_j \int_0^1 w(t S_j) \, \mathrm{d}t.$$

The above equation allows us to compute the m_1 monopolar source moments (λ_j) by taking m_1 suitable analytic functions ω_l, $1 \leqslant l \leqslant m_1$ and by solving the corresponding linear system of equations.

A possible trick, in order to get more information about the location of monopolar sources, is to compute rational approximants to the derivative of h_- on T_2, which is a rational function of degree m_1 that belongs to $L^2(T_2)$—thus to $\bar{H}_0^2$—for smooth enough boundary data ($\phi \in L^2(T_2)$ is enough). The related numerical trials are illustrated by figure 6 which indicates that this indeed allows us to localize the monopolar sources and to recover their moments, in cases without too much noise.

4.1.3. Mono/di-polar sources, $m_1, m_2 \neq 0$. The above schemes also allow us to treat these mixed cases as shown in figure 7 (also for noisy data).

As noted in sections 4.1.1 and 4.1.2, we recover the dipolar sources but we only get weak information about the monopolar ones. So, once the dipoles and their parameters (m_2, p_k and C_k) are identified, it would be possible to compute, as in section 4.1.2, the best rational
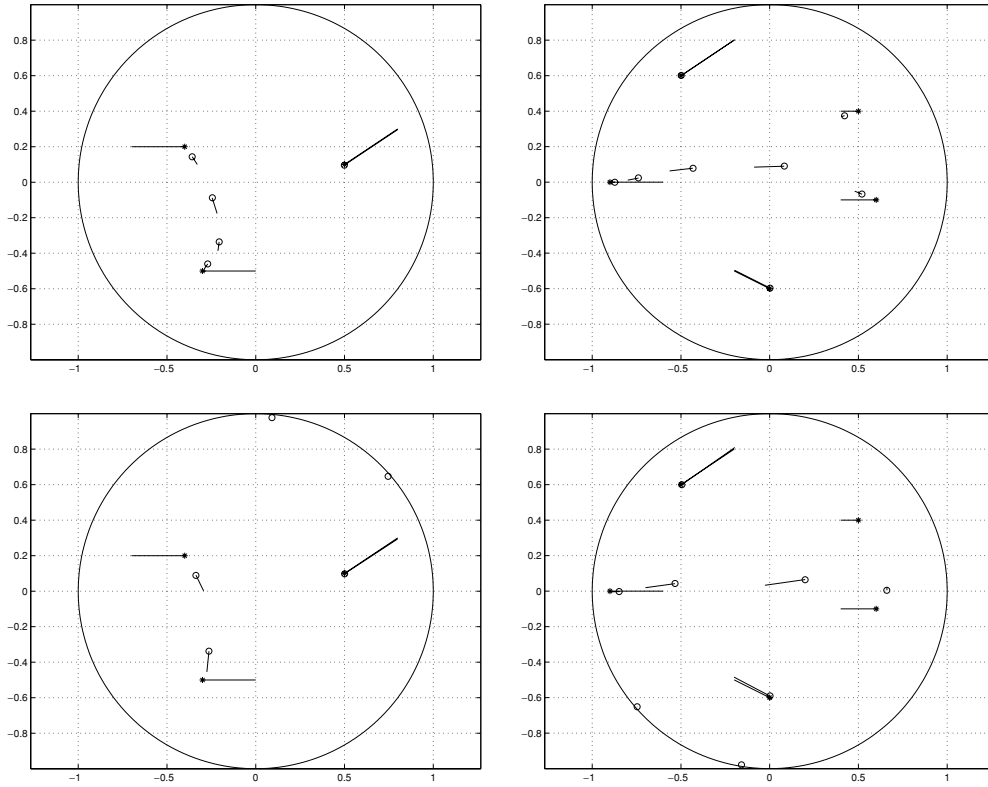
Figure 7. $m_1 = 2, m_2 = 1, n = 5$; $m_1 = 3, m_2 = 2, n = 8$; with noise 0% and 1%.

approximation to the derivative of the function $h_- - \sum_{k=1}^{m_2} \frac{p_k}{2\pi(z-C_k)}$, which is rational of degree m_1 with simple poles.

4.2. Small size inclusions

We now want to detect regular inclusions of small size ε, scattered in a matrix phase of known background conductivity, taken to be equal to 1. Consider then the function $f_\varepsilon - C_\varepsilon$ whose expression is given by (23) or (24) and whose trace on T_2 is computed from (22). For our numerical tests, the imposed boundary current flux is $\phi(\theta) = \cos\theta$. This implies that the corresponding background voltage potential is $u(z_1, z_2) = z_1 = r\cos\theta$ with $z_1 + iz_2 = r\,e^{i\theta}$. The potential u_ε is numerically generated by solving the direct Neumann problem (5) using a finite element method. We take 500 uniformly spaced points on the outer boundary T_2.

Because the underlying functions f_ε (23) or (24) are close to meromorphics, the best approximation method allows us to determine the number and the locations of the inclusions. Indeed, the number m of inhomogeneities is *a priori* unknown. If we look for a rational approximant of degree $n > m$, it has $n - m$ poles of null residue. The procedure is then to increase n until we only obtain poles with null moment (residue), and to keep m equal to the largest value of n providing a non-vanishing residue. Moreover, if the conductivities are known and the imperfections are well separated discs, their size could be computed too, since
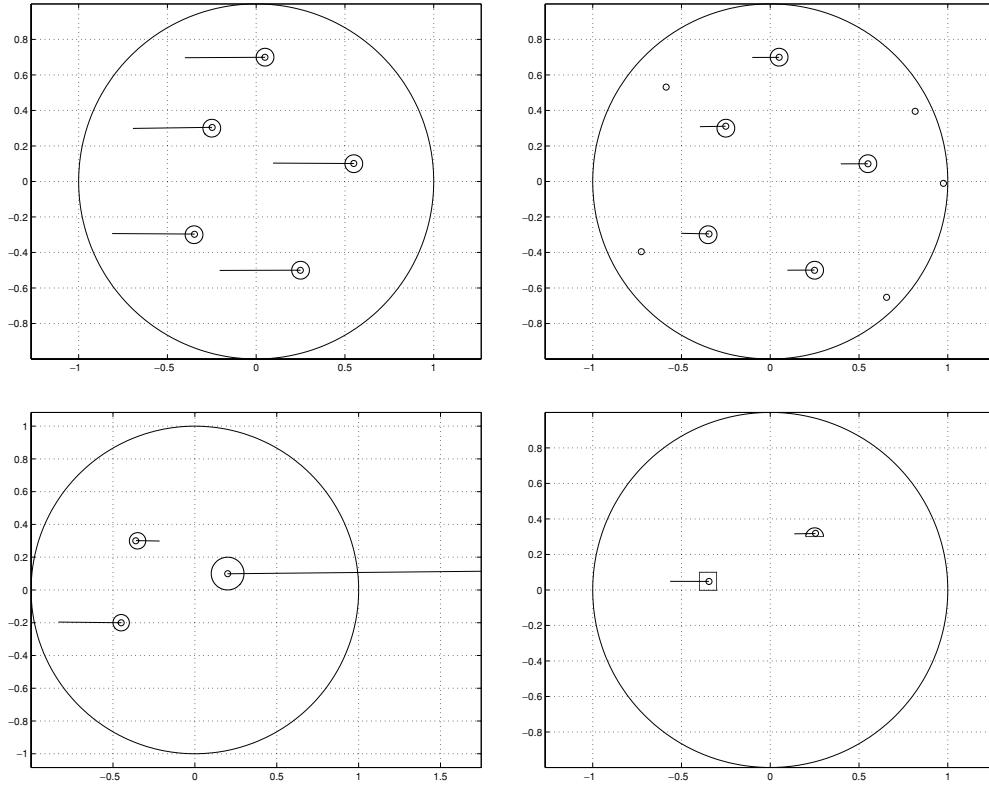
Figure 8. $m = 5$ identical discs, $n = 5, 10$; $m = n = 3$ discs; $m = n = 2$ inclusions.

we have the following relation between the fibre's size, its conductivity k_j and the residue r_j of the corresponding pole:

$$r_j = \frac{\varepsilon^2}{\pi} a_{11}^{(j)} = \varepsilon^2 \frac{1 - k_j}{1 + k_j},$$

from (18), (23). This is due to the particular choice of g which implies that $\nabla u(z) = \binom{1}{0}$, $\forall z \in \Omega$.

The recovered poles are represented by o. Their moments (residues) are designated by a line. They are symbolized by a dot when equal to 0. The domain is the unit ball B_2 and the small discs are the inclusions.

In the first two plots of figure 8, the domain contains five well-separated circular imperfections of radius 0.05 and conductivity 10. We see that they are well detected even in the case where their number is *a priori* unknown. Our method is also accurate for other geometries of the inclusions, as shown in the last two plots of figure 8 where we consider, in the third test, a domain containing three circular imperfections of radii 0.1, 0.05 and 0.05 and corresponding conductivities 0.1, 0.5 and 10, and, in the fourth one, a domain containing both a square and a half-disc inclusion.

In the first two plots of figure 9, we clearly see that for a configuration with two close circular inclusions of radius 0.05 and conductivity 10, separated by a distance equal to 0.02, the interaction is very strong so that we detect one equivalent conductivity imperfection as suggested by formula (24). This is also the case for touching inclusions as shown in the third
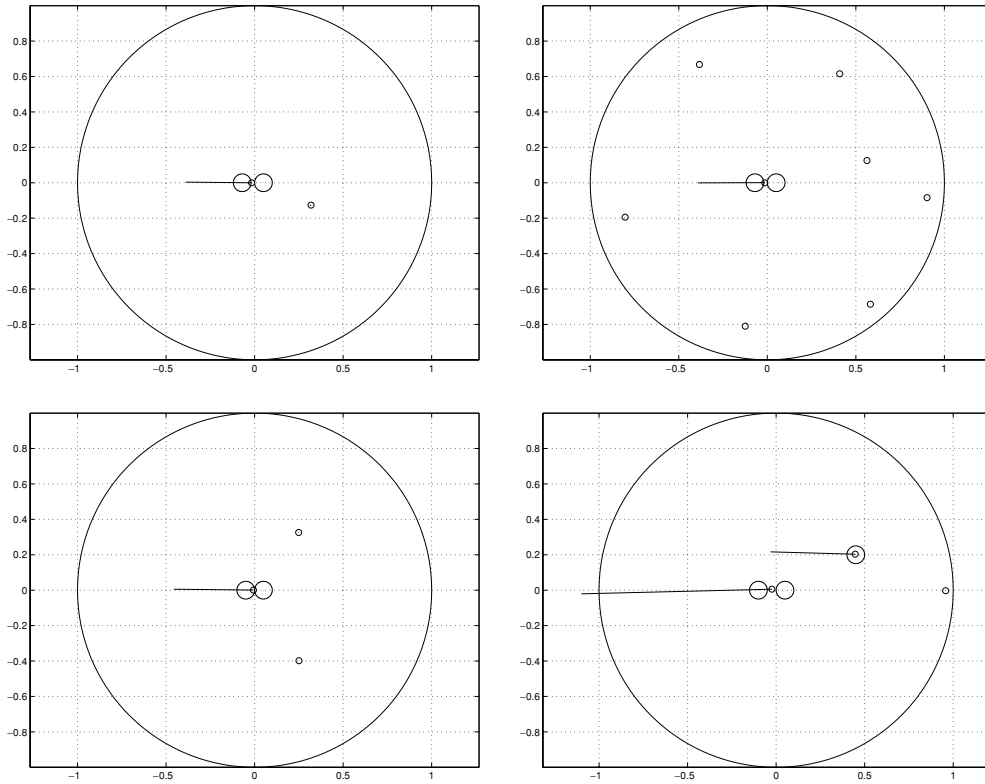
Figure 9. $m = 2$ close discs; $m = 2$ tangent discs; $m = 3$ discs, among which 2 close.

plot of figure 9 and, in the last picture, for a mixed situation with two close inclusions and an additional separated one, which does not interact too much with the others.

The location of the centres of circular inclusions, for a configuration with three inclusions of area $\pi \times 10^{-2}$ and conductivity equal to 10, are found with an error equal to 2.2×10^{-3}. It is equal to 3.5×10^{-3}, for five inclusions.

This error decreases as the contrast $1/k_i$ between the background conductivity and the conductivities of the inclusions approaches zero (for metals) and increases (for plastic). In fact, for a domain containing three inclusions, it is equal to 1.5×10^{-2} when the contrast is equal to $1/2$ and to 1.6×10^{-3} for a contrast of $1/50$.

This algorithm, applied for the detection of inclusions, is very sensitive to noise, since the pole residues are very small, of order ε^2. The example associated with figure 10 consists of a domain containing two inclusions, of radius 0.1 and conductivity equal to 50. The results are obtained using data without noise and with 0.1%, 1% and 5% respectively.

5. Comments

This work shows that rational or meromorphic approximation techniques provide tools for solving inverse problems of detecting and locating pointwise conductivity defaults or small inhomogeneities in 2D domains from complete overdetermined boundary data for the Laplace equation. Such problems originate from biomedical applications, issues in the environment,
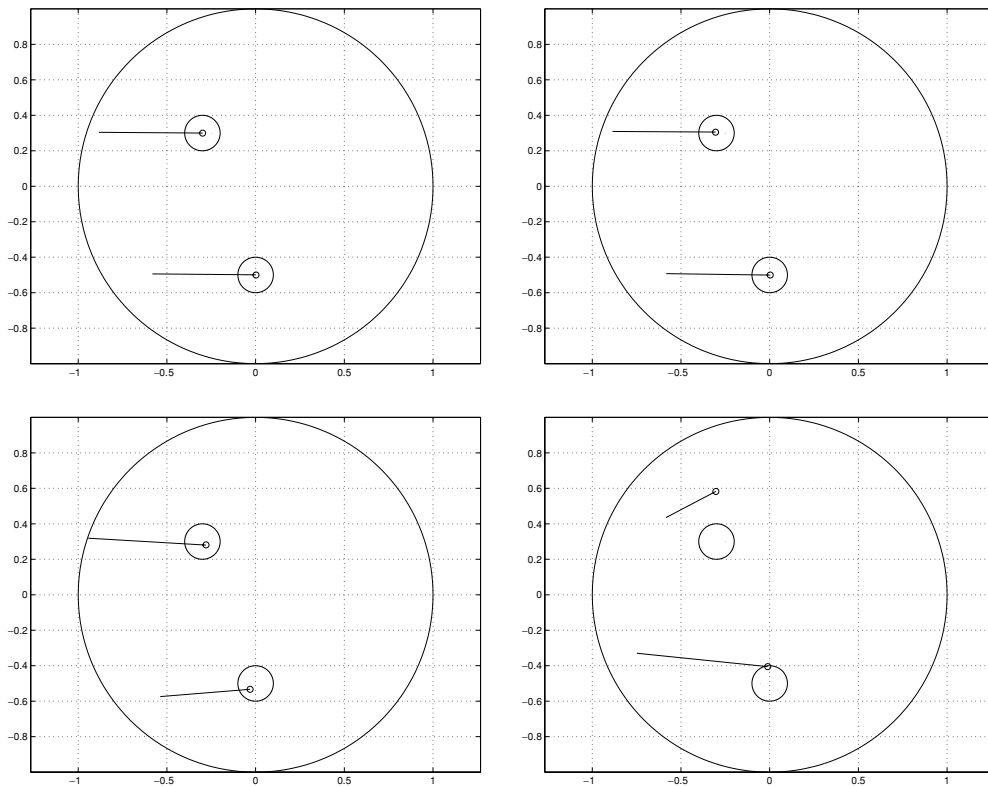
Figure 10. $m = 2$ with 0%, 0.1%, 1% and 5% noise.

such as the detection of polluting sources, or in structural mechanics. These tools should also be valuable to establish stability properties in Hardy–Sobolev spaces as in [22].

However several related issues remain to be explored, of which we list only two. The first one appears in the realistic situation where the available boundary data are incomplete (for instance, when the solution is measured on a strict subset of the boundary). One then needs either to recover the missing data or else to directly run singularity recovery schemes from partial data. Both strategies may be addressed as bounded extremal problems, as in [8, 16], which provides an approach at a very low computational cost. The second issue that we want to mention is the propagation of (possibly incomplete) outer Cauchy data to interior interfaces which are needed for EEG problems (2). This could in principle be handled using best approximation tools in Hardy classes of an annulus described in [17].

A 3D recovery algorithm for pointwise sources in a ball, that dwells on the 2D approach of the present paper, is currently under study [9]. It consists in solving for a sequence of 2D problems obtained by intersecting the ball with a family of planes. Indeed, the trace of the anti-harmonic part u_e of the 3D solution on the boundaries of planar cross sections of the ball B_3 (circles) admits expression as a function of two real variables, hence of the complex variable. The singularities of this family of functions are then related to those of the function u_e itself, while they can be computed in each disc as in a classical 2D situation. Preliminary experiments indicate that it is performing well enough. The case of more general 3D domains with parametrized boundary, those for which the plane cross sections are conformally equivalent to the disc, can also be handled that way, see [37] where

computations are done for ellipsoids. To our knowledge, genuine 3D best approximation tools are yet not available for bounded harmonic nor 'analytic' functions (following [52], a vector field in $\mathbb{R}^3$ would be called analytic if it is the gradient of a harmonic function). Finally, it is to be hoped that the techniques of the present paper could also be used in other contexts, for instance the Helmholtz equation.

Acknowledgment

References

[1] Adamjan V M, Arov D Z and Krein M G 1971 Analytic properties of Schmidt pairs for a Hankel operator and the generalized Schur–Takagi problem *Math. USSR Sbornik* **15** 31–73

[2] Ammari H, Bao G and Fleming J 2002 An inverse source problem for Maxwell's equations in magnetoencephalography *SIAM J. Appl. Math.* **62** 1369–82

[3] Ammari H, Moskow S and Vogelius M 2003 Boundary integral formulas for the reconstruction of electromagnetic imperfections of small diameter *ESAIM: Cont. Opt. Calc. Var.* **9** 49–66

[4] Ammari H and Seo J K 2003 An accurate formula for the reconstruction of conductivity inhomogeneities *Adv. Appl. Math.* **30** 679–705

[5] Andrieux S and Ben Abda A 1996 Identification of planar cracks by complete overdetermined data: inversion formulae *Inverse Problems* **12** 553–64

[6] Baratchart L 1986 Existence and generic properties for L^2 approximants of linear systems *IMA J. Math. Control Identif.* **3** 89–101

[7] Baratchart L, Cardelli M and Olivi M 1991 Identification and rational L^2 approximation: a gradient algorithm *Automatica* **27** 413–8

[8] Baratchart L, Leblond J, Mandréa F and Saff E B 1999 How can the meromorphic approximation help to solve some 2D inverse problems for the Laplacian? *Inverse Problems* **15** 79–90

[9] Baratchart L, Leblond J and Marmorat J-P Sources identification in 3D balls using meromorphic approximation in 2D disks, in preparation

[10] Baratchart L, Küstner R and Totik V 2004 Zero distribution via orthogonality *INRIA Research Report* 5291 submitted

[11] Baratchart L, Mandréa F, Saff E B and Wielonsky F Asymptotic behaviour of poles of rational and meromorphic approximants: application to 2D inverse problems for the Laplacian, in preparation

[12] Baratchart L and Olivi M 1988 Index of critical points in L^2-approximation *Syst. Control Lett.* **10** 167–74

[13] Baratchart L, Olivi M and Wielonsky F 1992 On a rational approximation problem in the real Hardy space H_2 *Theor. Comput. Sci.* **94** 175–97

[14] Baratchart L and Seyfert F 2002 An L^p analog to AAK theory for $p \geqslant 2$ *J. Funct. Anal.* **191** 52–122

[15] Begehr H G W 1994 *Complex Analytic Methods for Partial Differential Equations* (Singapore: World Scientific)

[16] Ben Abda A, Kallel M, Leblond J and Marmorat J-P 2002 Line-segment cracks recovery from incomplete boundary data *Inverse Problems* **18** 1057–77

[17] Ben Abda A, Leblond J, Mahjoub M and Partington J R Analytic extensions and Cauchy-type inverse problems on annular domains. I: Theoretical aspects and stability results submitted

[18] Ben Hassen F and Bonnetier E Asymptotic formulas for the voltage potential in a composite medium containing close or touching disks of small diameter *SIAM J. Multiscale Methods Simul.* at press

[19] Bonnetier E and Vogelius M 2000 An elliptic regularity result for a composite medium with 'touching' fibers of circular cross-section *SIAM J. Math. Anal.* **31** 651–77

[20] Bruhl M, Hanke M and Vogelius M 2003 A direct impedance tomography algorithm for locating small inhomogeneities *Numer. Math.* **93** 635–54

[21] Cannon J R and Ewing R E 1975 The locations and strengths of points sources *Improperly Posed Boundary Value Problems (Research Notes in Mathematics* vol 1*)* (London: Pitman) pp 39–53

[22] Chaabane S, Fellah I, Jaoua M and Leblond J 2004 Logarithmic stability estimates for a Robin coefficient in 2D Laplace inverse problems *Inverse Problems* **20** 47–59

[23] Chafik M, El Badia A and Ha-Duong T 2000 On some inverse EEG problems *Inverse Problems Eng. Mech.* II 537–44

[24] Chen G and Zhoua J 1992 *Boundary Element Methods* (New York: Academic)

[25] Cheney M, Isaacson D and Newell J C 1999 Electrical impedance tomography *SIAM Rev.* **41** 85–101

[26] Colton D and Kirsch A 1996 A simple method for solving inverse scattering problems in the resonance region *Inverse Problems* **12** 383–93

[27] Dautray R and Lions J-L 1987 *Analyse Mathématique et Calcul Numérique* vol 2 (Paris: Masson)

[28] Duren P L 1970 *Theory of H^p Spaces* (New York: Academic)

[29] El Badia A and Ha-Duong T 2000 An inverse source problem in potential analysis *Inverse Problems* **16** 651–63

[30] El Badia A and Ha-Duong T 2002 On an inverse source problem for the heat equation, with application to identifying a pollutant source *J. Inverse Ill-Posed Problems* **10** 585–99

[31] Faugeras O *et al* 1999 The inverse EEG and MEG problems: the adjoint state approach. I: The continuous case *INRIA Research Report* 3673

[32] Fengya D J, Moskow S and Vogelius M 1998 Identification of conductivity imperfections of small diameter by boundary measurements. Continuous dependence and computational reconstruction *Inverse Problems* **14** 553–95

[33] Garnett J B 1981 *Bounded Analytic Functions* (New York: Academic)

[34] Gilbard D and Trudinger N S 1983 *Elliptic Partial Differential Equations of Second Order (Grundlehren Math Wiss.* 224*)* (Berlin: Springer)

[35] Grisvard P 1985 *Elliptic Problems in Nonsmooth Domains* (Paris: Pitman)

[36] Hämäläinen M, Hari R, Ilmoniemi J, Knuutila J and Lounasmaa O V 1993 Magnetoencephalography—theory, instrumentation, and applications to noninvasive studies of the working human brain *Rev. Mod. Phys.* **65** 413–97

[37] Helme F O 2004 Résolution de problèmes inverses de sources dans des domaines paramétrés en dimension 3 par approximation méromorphe *DEA (MA) Report* University of Aix-Marseille

[38] Henrici P 1993 *Applied and Computational Complex Analysis* vol 3 (New York: Wiley-Interscience)

[39] Hoffman K 1988 *Banach Spaces of Analytic Functions* (New York: Dover)

[40] Kozlov V A, Maz'ya V G and Fomin A V 1991 An iterative method for solving the Cauchy problem for elliptic equations *Comput. Math. Phys.* **31** 45–52

[41] Küstner R 2003 Distribution asymptotique des zéros de polynômes orthogonaux par rapport à des mesures complexes ayant un argument à variation bornée *PhD Thesis* Université de Nice-Sophia Antipolis

[42] Kwon O, Seo J K and Yoon J R 2002 A real-time algorithm for the location search of discontinuous conductivities with one measurement *Commun. Pure Appl. Math.* **55** 1–29

[43] Li Y and Vogelius M 2000 Gradient estimates for solutions of divergence form elliptic equations with discontinuous coefficients *Arch. Rat. Mech. Anal.* **153** 91–151

[44] Lions J-L and Magenes E 1968 *Problèmes aux Limites Non Homogènes et Applications* vol 1 (Paris: Dunod)

[45] Mandréa F 2001 Comportement asymptotique des pôles d'approximants rationnels et méromorphes: application aux problèmes inverses du Laplacien 2D *PhD Thesis* Université de Nice-Sophia Antipolis

[46] Marmorat J-P, Olivi M, Hanzon B and Peeters R L M 2002 Matrix rational H^2 approximation: a state-space approach using Schur parameters *Proc. CDC'02 (Las Vegas, NV)*

[47] Miller K 1970 Stabilized numerical prolongation with poles *SIAM J. Appl. Math.* **18** 346–63

[48] Nečas J 1967 *Les Méthodes Directes en Théorie des Équations Elliptiques* (Paris: Masson)

[49] Peller V V 1991 Hankel operators and continuity properties of the operators of best approximation *Leningrad Math. J.* **2** 139–60

[50] Peller V V 2003 *Hankel Operators and Their Applications* (Berlinm: Springer)

[51] Pólya G and Szego G 1951 *Isoperimetric Inequalities in Mathematical Physics* (Princeton, NJ: Princeton University Press)

[52] Stein E M 1970 *Singular Integral Equations and Differentiability Properties of Functions* (Princeton, NJ: Princeton University Press)

[53] Vessela S 1992 Locations and strengths of point sources: stability estimates *Inverse Problems* **8** 911–7

[54] Young N J 1988 *An Introduction to Hilbert Space* (Cambridge: Cambridge University Press)